ELSEVIER

Chemical Geology 164 (2000) 81–92

CHEMICAL GEOLOGY
INCLUDING
ISOTOPE GEOSCIENCE

www.elsevier.com/locate/chemgeo

Fluorite $^{87}Sr/^{86}Sr$ and REE constraints on fluid–melt relations, crystallization time span and bulk D^{Sr} of evolved high-silica granites. Tabuleiro granites, Santa Catarina, Brazil

Ricardo Sallet [a,*], Robert Moritz [b], Denis Fontignie [b]

[a] *Department of Geology, Federal University of Rio Grande do Norte, CP 1639 59072-970 Natal RN, Rio Grande do Norte, Brazil*
[b] *University of Geneva, Switzerland*

Received 1 October 1998; accepted 7 June 1999

Abstract

The evolved high-silica Tabuleiro granites within the Early Paleozoic Santa Catarina Composite Massif, Pelotas Batholith, southern Brazil are characterized by the presence of euhedral to subeuhedral accessory fluorite and geochemical features typical of topaz–rhyolites and related A-type granites. Sr isotopes and REE data of the Tabuleiro granites and their accessory fluorite are used to constrain fluid–melt relations, crystallization time span and bulk crystal–melt Sr partition coefficient D^{Sr}.Correlations involving REE, Eu/Eu*, Rb/Sr, Sr and $^{87}Sr/^{86}Sr$ in fluorite and fluorite-host granites show that fluorite records the differentiation trend of the host Tabuleiro granites. REE-normalized patterns and Eu/Eu* relations in fluorite-bearing granites indicate that fluorite forms after the crystallization of the quartzo-feldspathic framework in residual melts. The Tabuleiro accessory fluorites yield high and variable $^{87}Sr/^{86}Sr$ ratios between 0.72334 and 0.8192. These ratios are neither the result of fluorite precipitation from a fluid nor Sr isotopic resetting. They result from ^{87}Rb decay in fluorine-rich high-Rb/Sr melts evolved by fractional crystallization in a magmatic system with a long crystallization time-span. Melt residence times of 300 to 700 ka and D^{Sr} of 4.7 to 6.0 are necessary to yield the high fluorite $^{87}Sr/^{86}Sr$ ratios. These results are compatible with those deduced elsewhere from high-silica rhyolitic volcanic equivalents.

Keywords: Fluorite; REE; Sr isotopes; Granites; Fluid

1. Introduction

Fluorine-rich high-silica topaz rhyolites and their corresponding A-type granites have fluorite as a characteristic accessory phase (Burt et al., 1982; Collins et al., 1982; Christiansen et al., 1983; Whalen et al., 1987). In this setting, fluorite is believed to precipitate during magmatic and/or magmatic–hydrothermal stages (Huspeni et al., 1984; Congdon and Nash, 1988; Johnston and Chappel, 1992; Price et al., 1992; Nash, 1993; Webster and Duffield, 1994). Despite the relatively abundant petrological data on fluorine-rich high-silica rhyolites and granites, the stability conditions and genesis of the accessory fluorite are poorly constrained.

The main question concerning the fluorite formation within evolved high-silica rhyolites and granites

* Corresponding author. Fax: +55-84-215-3806; E-mail: sallet@geologia.ufrn.br

0009-2541/00/$ - see front matter
PII: S0009-2541(99)00143-6

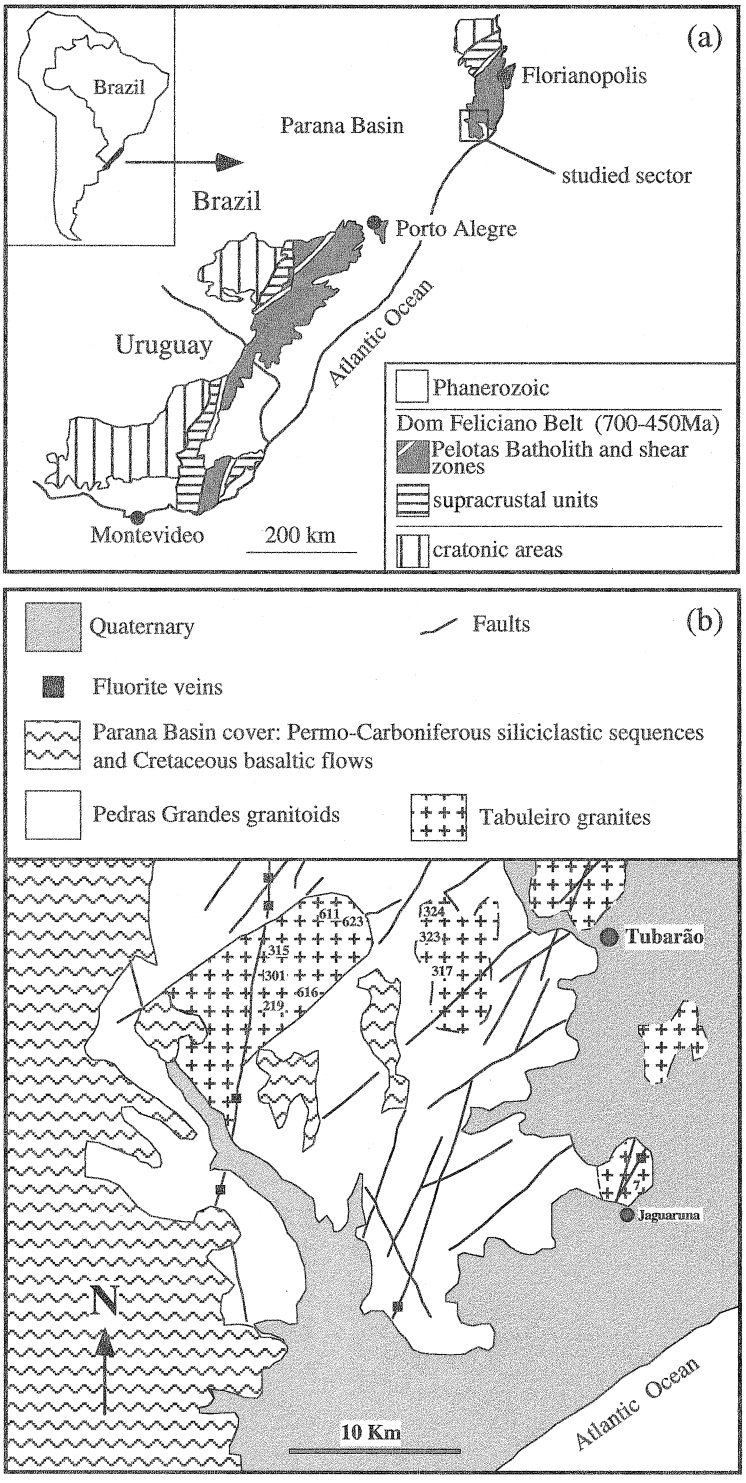
(a)
Brazil
Florianopolis
Parana Basin
studied sector
Brazil
Porto Alegre
Uruguay
Atlantic Ocean
Phanerozoic
Dom Feliciano Belt (700-450Ma)
Pelotas Batholith and shear zones
supracrustal units
cratonic areas
Montevideo
200 km
(b)
Quaternary
Faults
Fluorite veins
Parana Basin cover: Permo-Carboniferous siliciclastic sequences and Cretaceous basaltic flows
Pedras Grandes granitoids
Tabuleiro granites
611
623
315
301
616
219
324
323
317
Tubarão
Jaguaruna
N
10 Km
Atlantic Ocean

is whether it formed under supersolidus conditions from a silicate melt or from a magmatic–hydrothermal fluid, or under subsolidus conditions from a post-magmatic fluid. Experimental data on fluorite-bearing topaz rhyolite vitrophyre from the Spor Mountain, UT, USA, has shown that fluorite is stable under supersolidus conditions (Webster et al., 1987; Tsareva et al., 1992) and that, with low water contents, fluorite and biotite are late-stage phases (Webster et al., 1987).

Fluorite may be used to trace magmatic to magmatic–hydrothermal processes as REE and Sr substitute for Ca in fluorite. It is well known that fluorite may concentrate REE from the melt or fluid from which it crystallizes (Mineyev, 1969; Marchand et al., 1976; Tsareva et al., 1992). On the other hand, fluorite has very low Rb/Sr ratios which allows us to determine the $^{87}Sr/^{86}Sr$ ratios of the melt or fluid from which it precipitated.

The Tabuleiro high-silica granite, Santa Catarina, Brazil, is a favorable rock to study the geochemistry of accessory fluorite because medium-grained and relatively abundant purple fluorite is present. In this study, we use for the first time the Sr isotope and REE geochemistry of accessory fluorites and of their host granites to understand the formation of the accessory fluorite. Our new data allow us to set tighter constraints on fluid–melt relations, the crystallization time span and the bulk distribution coefficient D^{Sr} of evolved high-silica magmatic systems.

2. Geologic setting

The Early Paleozoic Santa Catarina Composite Massif is located along the northeastern extremity of the Pelotas Batholith in the Dom Feliciano Orogenic Belt of southern Brazil (Fragoso Cesar et al., 1986; Sallet et al., 1989) (Fig. 1a). Regional mapping has defined three plutonic associations in the massif, namely: the Valssungana, the Pedras Grandes and the Tabuleiro associations (Horbach and Marimon, 1982; Kirchner and Morgental, 1983).

In the southernmost sector of the massif, there are two well-defined major granitoid associations, based on distinctive textural, mineralogical and geochemical features: the subalkaline-monzonitic Pedras Grandes granitoids and the alkaline high-silica Tabuleiro granites (Sallet, 1988; Sallet et al., 1990, 1997) (Fig. 1b). The Pedras Grandes association comprises essentially coarse to medium-grained biotite-bearing (seldom hornblende) granites with considerable textural variation. Small dioritic to granodioritic interior bodies as well as fine-grained mafic enclaves are typically observed. The Tabuleiro association comprises medium to fine-grained, equigranular leucocratic biotite-bearing granites. Interstitial purple fluorite is usually observed with naked eye. These granites are devoid of mafic encalves.

Precise field and isotopic age relations between these two associations are still unknown. Nevertheless, regional mapping suggests a fault-controled emplacement of Tabuleiro granites within the Pedras Grandes granites (Horbach and Marimon, 1982; Kirchner and Morgental, 1983; Sallet, 1988) (Fig. 1b). Chemical trends of the two associations also suggest that the Tabuleiro granites are younger than the Pedras Grandes granites (Sallet et al., 1990, 1997). In fact, the alkaline high-silica association is related to late to post-tectonic processes whereas the subalkaline-monzonitic association is usually related to late-tectonic magmatic processes (Batchelor and Bowden, 1985)

Permo-Carboniferous siliciclastic sedimentary sequences and Early Cretaceous continental basalt flows from the Parana Basin cover the massif on its western edge and crop out within the massif. Post-Jurassic fluorite-chalcedony veins of the Santa Catarina Mining District are hosted by faults affecting the granitoids (Sallet et al., 1996) (Fig. 1b).

3. Analytical methods

Tabuleiro granite samples with visible purple fluorite and weighing 10 to 20 kg were collected from

Fig. 1. (a) Geotectonic setting of the Pelotas Batholith with the Santa Catarina Composite Massif located along its northeastern extremity (Sallet et al., 1990). (b) Geological map of the southernmost sector of the Santa Catarina Composite Massif (adapted from Horbach and Marimon, 1982, Kirchner and Morgental, 1983 and Sallet, 1988). Numbers are sample locations.

road cuts. Granite analyses were performed at the University of Lausanne, Switzerland, by X-ray fluorescence (XRF) for major and trace elements and by inductively coupled plasma-atomic emission spectrometry (ICP-AES) for REE. F was determined by specific ion electrode at the C.R.P.G, Nancy, France. Li was analyzed by atomic absorption spectrometry (AAS) and Sn by inductively coupled plasma-mass spectrometry (ICP-MS) at XRAL Laboratories, Ontario, Canada.

Accessory fluorite grains were separated from five samples. After crushing, the $-0.25+0.63$ mm granulometric fraction was selected. Felsic concentrates were obtained using an electromagnetic separator. Fluorite was separated from the felsic concentrates using bromoform, and thereafter, purified carefully by handpicking under a binocular microscope. The final concentrates weighed between 100 and 150 mg. REE and trace elements analyses were performed at the C.R.P.G. by ICP-MS. Additional major elements (ICP-AES) and F (specific ion) analysis on two concentrates were carried out to estimate their purity (Table 1). Assuming that all Ca is present as fluorite, stoichiometric calculations point to 91.5 a 94.1% fluorite in the two analyzed concentrates. The main impurities are SiO_2, Al_2O_3, Fe_2O_3, P_2O_5 and ΣREE_2O_3. Considering that a fraction of these elements may be present in fluorite as diadochic substitution, the stoichiometric amount of calculated fluorite should be considered as the minimum percent of fluorite present in the concentrates.

Table 1
Major elements composition (wt.%) for the fluorite concentrates
ICP-AES precisions for majors elements are better than: 2% for CaO; 5% for Fe_2O_3; 10% for SiO_2, Al_2O_3, Na_2O and K_2O; 20% for P_2O_5.
Specific ion electrode precision for F is better than 2%.

	T616	T623b
SiO_2	4.07	3.75
Al_2O_3	1.36	1.12
Fe_2O_3	1.58	0.35
MnO	0.04	n.d.
MgO	0.20	0.15
CaO	65.81	67.62
Na_2O	0.19	0.18
K_2O	0.18	0.27
TiO_2	0.13	0.05
P_2O_5	0.37	0.99
ΣREE_2O_3	1.29	0.81
F	42.82	42.78
F=O	18.03	18.01
Total	100.01	100.06

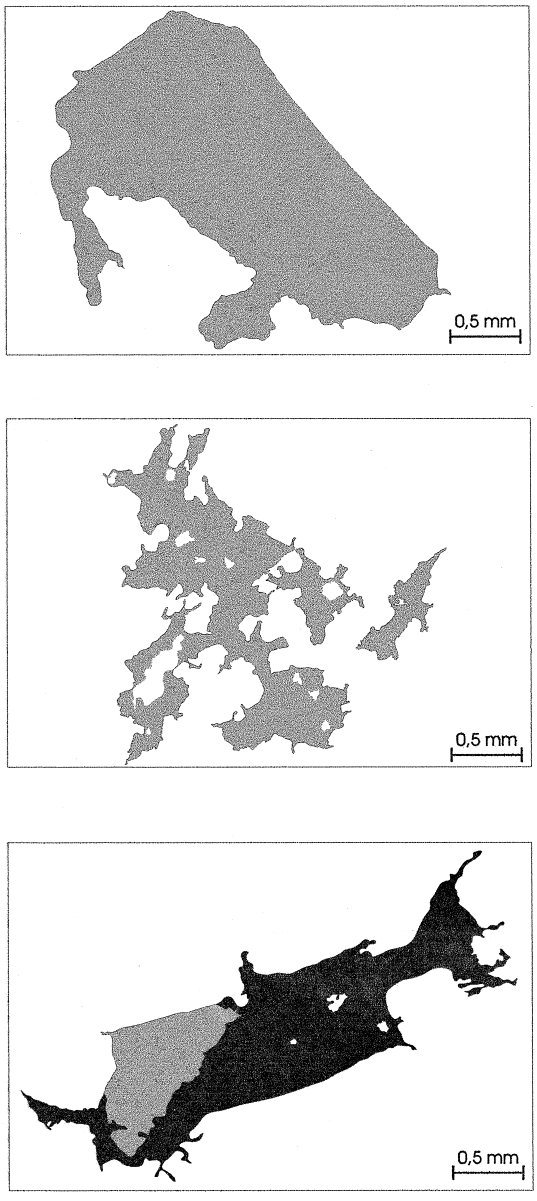

Fig. 2. Microphotograph overlay drawing of typical fluorite crystals in Tabuleiro granites. The white area in each sketch represents the quartzo-feldspathic framework. The bottom sketch shows fluorite–biotite association.

Granites were dissolved in HF and fluorites were leached with HCl. Sr was separated by standard HCl ion-exchange columns, and Sr isotope ratios were measured at the University of Geneva, Switzerland, on a 7-collector Finnigan Mat 262 thermal ionisation mass spectrometer. $^{87}Sr/^{86}Sr$ ratios were measured in static mode and are mass fractionation corrected to an $^{87}Sr/^{86}Sr$ ratio of 8.375209 and normalized to the Eimer and Amend $SrCO_3$ standard = 0.708019 $\pm$ 6 (2SE) during the period the analyses of these samples were performed.

4. Petrography and geochemistry of the Tabuleiro granites

The Tabuleiro granites are chemically and mineralogically very similar to topaz rhyolites (Burt et al., 1982; Christiansen et al., 1983) and some A-type granites (Collins et al., 1982; Whalen et al., 1987). Sodic plagioclase, strongly perthitic alkali feldspar and quartz form an equigranular texture, locally porphyritic. Interstitial biotite almost completely transformed to chlorite and purple fluorite are late-stage phases. Fluorite occurs mainly as purple interstitial grains and occasionally as inclusions in feldspars (Fig. 2). Interstitial fluorite, locally associated with biotite, forms euhedral to subeuhedral crystals within the quartzo-feldspathic framework. Minute mineral inclusions (< 50 μm) are sporadically observed in the fluorites. Among these, xenotime, fergusonite and bastnaesite-like fluorocarbonates could be identified by scanning electronic microscope (SEM) equipped with a X-ray detector working in energy dispersive spectrometry (EDS) (J.M. Montel, personal communication). Muscovite are seldom present, associate to feldspars and to chlorite. Topaz, molibdenite and zircon are local accessory phases.

Table 2
Whole rock chemical analyses of Tabuleiro granites. Oxydes in wt.%, trace elements in ppm
XRF precisions for trace elements are better than: 2.5% for Sr and U; 4% for Rb; 5% for Ga; 8% for Nb and Zr; 10% for Pb and Zn; 18% for Th. Specific ion electrode precision for F is better than 4%. AAS precision for Li is better than 5%. ICP-MS precision for Sn is better than 7%. nd — not detected; na — not analyzed.

	T317	T316	T623b	T301	T323	T219	T616	T324	T611a	T623a	T7	T315
SiO_2	74.83	75.56	75.59	75.8	76.29	76.5	76.72	77.07	77.11	77.14	77.68	77.77
TiO_2	0.05	0.06	0.11	0.04	0.04	0.04	0.06	0.05	0.05	0.04	0.04	0.07
Al_2O_3	11.97	12.23	12.51	12.88	12.15	13.18	12.54	12.88	12.56	12.51	12.94	12.57
Fe_2O_3	1.17	1.22	1.15	1.06	1.08	0.78	1.03	0.93	0.67	0.72	0.98	1.14
MnO	0.04	0.04	0.03	0.02	0.04	0.02	0.03	0.03	0.01	0.02	0.01	0.03
MgO	0.01	0.01	0.07	nd	nd	nd	0.04	nd	0.02	0.03	nd	0.07
CaO	0.44	0.58	0.63	0.6	0.44	0.54	0.57	0.59	0.41	0.43	0.46	0.43
Na_2O	3.86	3.51	3.28	4.03	3.69	3.98	3.69	3.78	4.2	4.12	4.23	3.52
K_2O	4.36	4.54	5.23	4.45	4.18	4.64	4.68	4.62	4.4	4.42	4.39	4.8
P_2O_5	nd	0.01	0.02	0.01	0.01	0.01	0.01	0.01	0.01	0.01	0.01	0.01
LOI	1.2	2.04	0.73	0.81	2.75	1.01	0.55	0.65	0.45	0.35	0.62	0.4
Total	97.93	99.8	99.54	99.7	100.67	100.7	99.92	100.61	99.89	99.78	101.36	100.81
Nb	5	3	30	26	5	37	46	21	35	27	23	nd
Zr	105	110	186	118	97	124	129	100	113	105	99	81
Y	70	123	105	200	69	119	135	125	92	77	138	65
Sr	9.2	7	20	4.4	1	8.7	11	7.5	3	5	2	22.6
U	nd	15	24	13	2	12	20	33	7	9	15	4
Rb	345	597	521	666	314	938	642	526	377	349	421	344
Th	33	47	54	45	19	50	50	48	40	39	41	26
Pb	24	37	48	56	2	62	59	51	24	33	58	nd
Ga	18	22	21	28	11	30	22	21	20	18	28	7
Zn	55	64	57	59	33	60	51	26	26	49	83	nd
F	2300	3700	3900	3800	2400	4600	3500	3200	2000	2400	1700	1300
Li	18	7	39	112	15	na	9	19	12	12	19	11
Sn	11	25	38	27	14	na	33	18	11	11	12	9

Chemical analyses of Tabuleiro granites are presented in Table 2. These granites, have SiO_2 increasing from 75 to 78% and the alkalinity index $\log(CaO/Na_2O + K_2O)$ varying from −1.30 to −1.0. They have a typically high-silica alkaline affinity of A-type granites and topaz rhyolites (Sallet et al., 1997). The aluminium saturation index, ASI = $Al/(K + Na + Ca)$, varies from 1.04 and 1.11 implying a slight peraluminous character for these granites. As commonly observed in evolved high-silica alkaline magmas (Christiansen et al., 1983; Webster and Duffield, 1991; Charoy and Raimbault, 1994; Sallet et al., 1997), major elements show narrow variations and low to very low Ca, Mg, Ti and P contents whereas trace elements span over an extended range with pronounced enrichments in Rb, Y, U, Th and Nb and very low Sr content. The ubiquitous presence of fluorite explains the high fluorine contents of the whole-rock analyses, between 1300 and 4900 ppm. The high F and Rb contents of these granites are characteristic of high-silica crustal-derived magmas (Sallet, 1999; Sallet et al., 1997). REE patterns are flat with strong negative Eu anomalies (Fig. 3a).

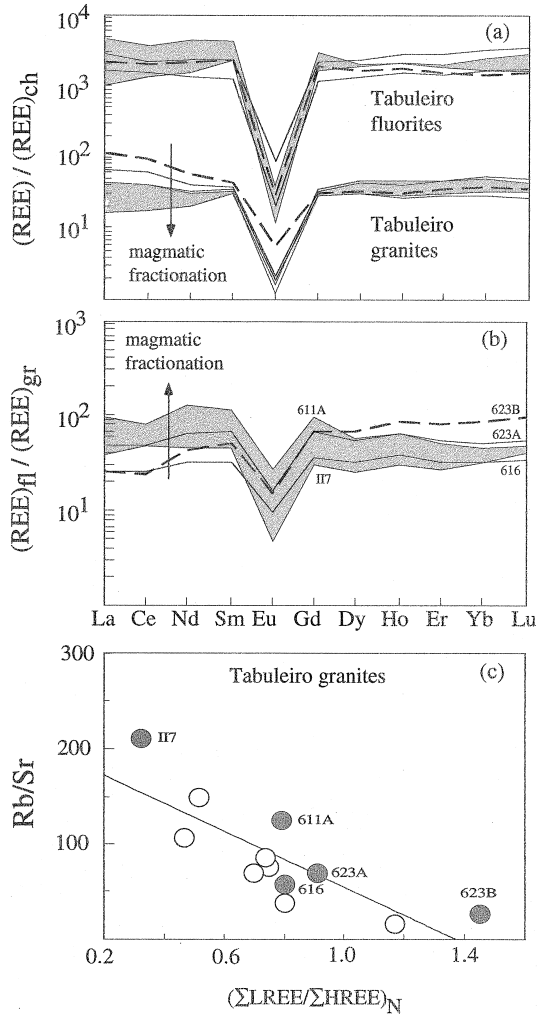

Fig. 3. (a) REE chondrite-normalized patterns of Tabuleiro granites and their accessory fluorite. Normalization values from Evensen et al. (1978) (b) REE pattern of accessory fluorite normalized to their host granites. (c) Rb/Sr vs. $(\Sigma LREE/\Sigma LHREE)_N$ diagram showing the Tabuleiro granites magmatic fractionation trend. Samples from which accessory fluorite and host granite were analyzed are labeled. The shaded area in (a) and (b) links the two more evolved granite samples T7 and T611A.

Rb–Sr isotope systematics of the Tabuleiro granites yield whole-rock errorchrons as is usually expected with very high Rb/Sr magmas (Mahood and Halliday, 1988; Gerstenberger, 1989). The ages determined for the Tabuleiro association are younger than the Rb–Sr age of 523 Ma yielded by the Pedras Grandes association (Sallet et al., 1996, 1997) and the initial $^{87}Sr/^{86}Sr$ ratios are abnormally high with values above 0.80. An errorchron (not shown) based on combined Rb–Sr data from accessory fluorite and the host granite gives an age of 442 ± 27 Ma, within the range of the whole-rock errorchron, with an initial $^{87}Sr/^{86}Sr$ ratio of 0.70 ± 0.07.

5. Tabuleiro granitic fluorites

5.1. REE and other lithophile elements

Other than REE, trace elements Be, Nb, Ta, U, Th and Zr are present in fluorite in significant amounts, between 75 and 1100 ppm (Table 3). This element association, probably accounted for by minute mineral inclusions in fluorite, is typically enriched in F-rich high-silica magmas forming topaz rhyolithes and A-type granites (Christiansen et al., 1983; Congdon and Nash, 1988; Webster and Duffield, 1991; Charoy and Raimbault, 1994).

Chief minerals carrying REE in granites are phosphates, niobotantalates, carbonates and zircon (Bea, 1996). Zircon and carbonates may be discarded as

significant mineral inclusions in the fluorite concentrates inasmuch as Zr is low and CO_2 is absent, as suggest by the 100% closure of the concentrate analyses (Tables 1 and 3). Maximum theoretical REE contributions from phosphates (monazite and xenotime) and niobotantalate (fergusonite) are estimated to be negligible and thus reported REE contents are accounted for only by fluorite (Table 4).

The REE data given in Table 3 are plotted in Fig. 3. The fluorites from the Tabuleiro association display higher REE concentrations than the whole rocks from which they were separated, but they have chondrite-normalized patterns that are very similar to those of their host granites (Fig. 3a). However, the granites have more dispersed LREE contents than the fluorites. This feature is also represented by the fluorite-host granite normalized REE patterns (Fig. 3b). With advancing melt fractionation, recorded by an increase in the Rb/Sr ratio, the granites display a decrease in the LREE/HREE ratio (Fig. 3a and c). However, an inverse relation is observed for the fluorite-to-host granite REE normalized pattern, namely an increase in LREE/HREE ratios as melt fractionation progresses (Fig. 3b). It means that fluorite is a late-stage phase and records the REE pattern of the feldspar-fractionated residual melt or magmatic fluid from which it crystallizes. As for other calcic phases, fluorite should have a higher Eu partition coefficient compared to the other REE. The more negative Eu anomalies in fluorite compared to

Table 4
Maximum theoretical REE contribution for the fluorite concentrates from phosphate and niobotantalate mineral inclusions
$(X)_{min}$ = mass fraction of mineral inclusion. Mass fractions are calculated by allocating maximum P_2O_5 and Nb contents of concentrates (Table 1, Table 3) to phosphates and niobotantalates, respectively.
$(X)_{REE}$ = maximum REE fraction of the concentrate carried by the inclusion minerals. Nd, Dy and Ce chosen for calculations as they are the most enriched REE in each of the minerals.
Typical mineral compositions used in calculations taken from Bea (1996).

	$(X)_{min}$, %	$(X)_{Nd}$, %	$(X)_{Dy}$, %	$(X)_{Ce}$, %
Fergusonite	0.29	0.02		
Xenotime	3.30		0.17	
Monazite	3.30			0.6

Table 3
REE and other trace element compositions (ppm) for Tabuleiro granites and fluorites
gr — granite, fl — fluorite. ICP-AES precisions for granites are 5–10%.
ICP-MS precisions for fluorites are: better than 5% for La, Ce, Nd, Sm, Ho, Tb, Yb, Lu; 5–12% for Eu; better than 6% for Gd; better than 7% for Dy. For other trace elements, precisions are better than 5%, excepted 7% for Th. na — not analyzed.

	T611A		T616		T623a		T623b		T7	
	gr	fl	gr	fl	gr	fl	gr	fl	gr	fl
La	15.9	1525	24.5	624	16.3	783.3	40.6	1074	6.3	241
Ce	38.1	3142	60.3	1511	39.5	1896	88.1	2125	17	820
Nd	22.3	2926	29.6	955.7	24	1589	39.8	1680	14.65	684
Sm	7.7	896.2	9	290.1	8.2	552.7	10	527.5	7.33	337
Eu	0.11	2.99	0.19	1.83	0.16	2.54	0.49	7.66	0.14	0.66
Gd	8.6	834.4	9.8	356.8	8.7	596.1	9.4	656.5	10.85	332
Dy	12	699	16.2	512.8	11.4	621.4	12.8	860.5	18	475
Ho	2.49	165.3	3.55	133.2	2.33	150	2.71	235.6	3.92	119
Er	7.9	418.2	11.6	369.4	7.1	383.4	8.8	711.1	11.88	327
Yb	8.3	377.5	12.9	408	7.2	364	9.4	805.1	12.66	400
Lu	1.22	59.43	1.87	62.52	1.06	58.2	1.36	130.8	1.68	70.63
Eu/Eu*	0.05	0.01	0.07	0.02	0.07	0.02	0.18	0.05	0.06	0.01
Be		86.2		75		52.9		117		42.51
Nb		493.6		176		414.8		458		224.96
Ta		49.01		42.76		34.35		74		na
Th		1094		562		967.8		890		597.8
U		111		87		100.7		134		42.85
Zr		286		185		327		365		130.95
Sn		34.2		15.22		23.4		15.22		na

those of the host granites (Fig. 3a and Table 3) means that feldspar crystallization depleted an already severely Eu-depleted magma or related fluid.

It has been shown experimentally that fluorine and REE enter the melt rather than the fluid in magmas which are not excessively fluorine rich (Webster, 1990; Keppler and Wyllie, 1991). These data agree with a crystallization from the melt. In this case, the matching granite and fluorite REE patterns within the Tabuleiro association can be explained by high and similar fluorite-magma REE partition coefficients. On the other hand, experimental data indicate that fluorine partitions preferentially into the fluid with increasing fluorine contents leading to fluorine-rich magmatic-hydrothermal systems (Webster, 1990; Keppler and Wyllie, 1991). Under such conditions, REE solubilities in hydrothermal fluids increase (Flynn and Burham, 1978; Webster, 1990) and the REE-fluid composition should approach the REE-melt composition. In this case, the matching fluorite and granite REE patterns of the Tabuleiro association may also be explained. Although experimental data (Flynn and Burham, 1978) indicate very low REE fluid–melt partition coefficients, extremely high fluorite–fluid REE partition coefficients may explain the elevated fluorite REE contents.

5.2. Sr isotopes

The Tabuleiro granitic fluorite has variable and high present day $^{87}Sr/^{86}Sr$ ratios between 0.7233 and 0.8192, and low $^{87}Rb/^{86}Sr$ ratios between 0.611 and 2.866 (Table 5). To reach such high values by $^{87}Rb-$ decay, time spans greater than 2 Ga would be necessary. The geological context of the Santa Catarina District clearly excludes this possibility (Horbach and Marimon, 1982; Kirchner and Morgental, 1983; Fragoso Cesar et al., 1986) and present-day high $^{87}Sr/^{86}Sr$ fluorite ratios cannot be taken as a homogeneous initial ratio for the Tabuleiro granites.

The influence of minute mineral inclusions observed in the granitic Tabuleiro fluorites on the measured isotopic ratios is minor since their $^{87}Rb/^{86}Sr$ ratios are very low. Low $^{87}Rb/^{86}Sr$ values may only be explained if occasional high-Rb/Sr included phases were present in very small fractions, implying a negligible contribution of radiogenic Sr. Thus, the time-evolution of a radiogenic mineral inclusion cannot explain the high $^{87}Sr/^{86}Sr$ ratios of the Tabuleiro fluorites.

Two main processes may account for the high $^{87}Sr/^{86}Sr$ fluorite ratios and their variations. The first one is ^{87}Sr growth by ^{87}Rb decay in high Rb/Sr residual melts during a long crystallization time-span. In such a scenario the residual melts are continuously enriched with ^{87}Sr during fractional crystallization and ^{87}Sr is retained in residual melt because the melt is not in isotopic equilibrium with the cumulating crystalline framework (Mahood and Halliday, 1988; Halliday et al., 1989, 1991; Christensen and DePaolo, 1993; Cavazzini, 1994). The second process could be fluorite formation from an exsolved high-Rb/Sr fluid phase or a resetting of the fluorite

Table 5
Rb, Sr and $^{87}Sr/^{86}Rb$ data for Tabuleiro granites and fluorites
gr — granite, fl — fluorite. XRF precisions for granites are better than: 4.0% for Rb; 2.5% for Sr. ICP-MS precisions for fluorites are better than: 8% for Rb; 5–10% for Sr.

		Rb (ppm)	Sr (ppm)	$^{87}Rb/^{86}Sr$	$^{87}Sr/^{86}Sr$	Error ($\pm$2SE)
T7	gr	421	4.42	888.15	4.332	2
	fl	13.34	14.54	2.69	0.8192	1
T611a	gr	377	3	475.73	3.8604	2
	fl	29.56	42.20	2.03	0.7943	2
T616	gr	642	11	182.77	1.5505	1
	fl	40.18	79.10	1.48	0.7533	3
T623a	gr	349	5	227.77	2.0147	8
	fl	14.14	50.70	0.81	0.7717	3
T623b	gr	521	20	79.49	1.2672	1
	fl	35.85	170	0.61	0.7233	8

$^{87}Sr/^{86}Sr$ ratio recorded at the magmatic stage by this fluid.

6. Fluid–melt relations

Fluorine-rich high-silica melts forming topaz rhyolites and their A-type granitic equivalents are considered to be relatively dry. The low water contents of these melts are related to their source rocks (Burt et al., 1982; Collins et al., 1982; Christiansen et al., 1983; Clemens et al., 1986; Creaser et al., 1991). Since water solubility is strongly enhanced by increasing fluorine contents in haplogranitic melts (Holtz et al., 1993), it is suggested that fluorine-rich high-silica melts are water undersaturated rather than saturated. The low water and high fluorine contents of these melts suggest that exsolution of a fluid

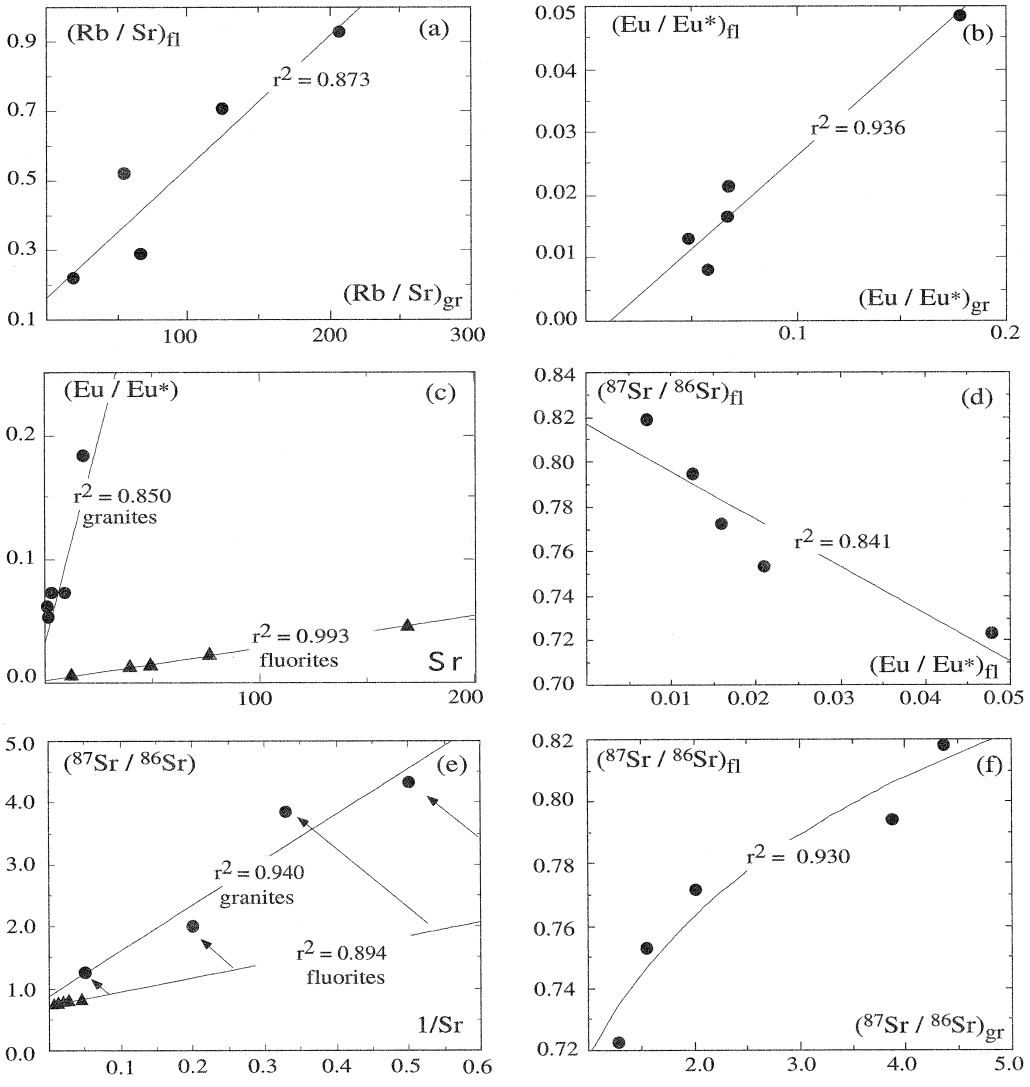

Fig. 4. (a) fluorite vs. host Tabuleiro granite Rb/Sr ratios. (b) fluorite vs. host Tabuleiro granite Eu/Eu* ratios. (c) Eu/Eu* vs. Sr diagram showing fluorite and host granites evolution. (d) Tabuleiro fluorite $^{87}Sr/^{86}Sr$ vs. Eu/Eu* evolution. (e) fluorite and host Tabuleiro granites evolution in the $^{87}Sr/^{86}Sr - 1/Sr$ diagram. (f) fluorite vs. host Tabuleiro granite $^{87}Sr/^{86}Sr$. r^2 Values are squared correlations coefficients.

phase could have occurred during late stage near solidus crystallization processes with low fluid–melt (crystals + melt) ratios. According to the experimental data of Clemens et al. (1986) and Webster et al. (1987), the low water content of the Tabuleiro melts is indicated by the biotite textural position suggesting a late crystallization stage (Fig. 2).

The fluorite and fluorite-host granite Rb/Sr, Sr, $^{87}Sr/^{86}Sr$, and Eu/Eu* relations show that fluorite clearly records the compositional evolution of the host granite (Fig. 4a,b,c,d). The good correlations shown in Fig. 4 may be explained by fluorite crystallizing from evolving silicate melts or, at least, from F-rich related fluids that would approach melt composition (Koster Van Gross and Wyllie, 1969; Keppler and Wyllie, 1991). However, if fluorite forms from, or reacts with, a chemically and isotopically single homogeneous hydrothermal fluid, it should record constant elemental and isotopic ratios. As fluid compositions in fluid–melt systems are still poorly constrained, the observed trends in Fig. 4 are thus better explained by considering that the Tabuleiro fluorite crystallized from a silicate melt.

The evolution of melt $^{87}Sr/^{86}Sr$ ratios and Sr contents during the fractional crystalization is described by a hyperbolic curve (Cavazzini, 1994). Thus, in a $^{87}Sr/^{86}Sr$–1/Sr diagram (Fig. 4e) the Tabuleiro fluorites display a positive linear correlation. As this trend is coherent with the whole REE, Eu/Eu*, Rb/Sr, Sr and $^{87}Sr/^{86}Sr$ correlations, interpreted as the result of melt fractionation, it should not be related to fluid mixing processes. Therefore, this trend is best interpreted as the result of successively more fractionated and more radiogenic residual melts from which fluorite was formed, recording progressively higher $^{87}Sr/^{86}Sr$ ratios.

7. Crystallization time span and bulk D^{Sr} constrains

The magmatic origin of the recorded $^{87}Sr/^{86}Sr$ ratios in fluorite is the only mechanism to explain all the observed chemical correlations. Formulations by Cavazzini (1994) indicate that to reach the high $^{87}Sr/^{86}Sr$ values recorded by the granitic fluorites by means of fractional crystallization, it is required that the Tabuleiro granites represent very low fractions of residual magmas evolved during long crystallization time spans. Using the following equation from Cavazzini (1994):

$$^{87}Sr/^{86}Sr = \left(^{87}Sr/^{86}Sr\right)_0 + \lambda R_0\left(^{87}Sr/^{86}Sr\right)_0 \times T(1 - F^{b+1})/(b+1)$$

where $\lambda = 1.42\ 10^{-11}\ a^{-1}$; $R_0 = (^{87}Rr/^{86}Sr)_0$; $T =$ time; $F =$ remaining melt fraction; $b = D^{Rb} - D^{Sr}$; we can graphically represent the relationships between crystallization time spans, and the bulk distribution coefficients D^{Rb} and D^{Sr} (Fig. 5). The more radiogenic fluorite with $^{87}Sr/^{86}Sr = 0.8192$ is taken to constrain the upper crystallization time span limit. It is reasonable to assume that the initial melt has a low $^{87}Rb/^{86}Sr$ ratio of 10 and that crystallization leads to a low remaining melt fraction F of 0.1. The initial Sr isotopic ratio varies between 0.70 and 0.75. It can be noted from the Cavazzini equation that the bulk D^{Sr} values strongly determine the growth rate of $^{87}Sr/^{86}Sr$. With bulk D^{Rb} values varying between 0.1 and 1.0 (e.g., Halliday et al., 1991) D^{Sr} values change between 6.75 and 7.75 and the melt reaches a $^{87}Sr/^{86}Sr$ ratio of 0.819 in 10 ka, which is the smallest crystallization time for silicic plutons

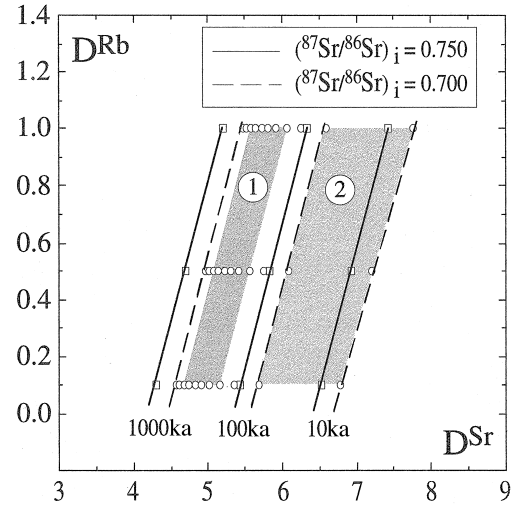

Fig. 5. Crystallization time spans, bulk partition coefficients D^{Rb} and D^{Sr} and $^{87}Sr/^{86}Sr$ evolution relations for fluorite. This diagram is constructed from the equation of Cavazzini (1994) (see text for explanation). Shaded areas show time spans derived from Sr isotopic data by Halliday et al. (1991) at the Long Valley silicic system (1) and from conductive heat loss and silicic pluton crystallization (2) (Lachenbruch et al., 1976; Spera, 1979).

cooling by conductive heat loss (Lachenbruch et al., 1976; Spera, 1979). Taking the calculated minimum time scales between 300 and 700 ka of the Long Valley silicic magmatic system (Halliday et al., 1989; Christensen and DePaolo, 1993), D^{Sr} values betwen 4.7 and 6.0 are required to explain the more radiogenic fluorite Sr isotope ratio. These values are consistent with the ones inferred for some high-silica systems by Halliday et al. (1991). Although the crystallization time span is poorly constrained, the high thermal gradient of the batholithic environment of the Tabuleiro granitic association precludes a simple cooling regime by conductive heat loss. Hence, the minimum crystallization time span of the Long Valley system (Halliday et al., 1989) is taken as a reference.

8. Conclusions

$^{87}Sr/^{86}Sr$ and REE ratios associated with textural features of the Tabuleiro granitic fluorite, indicate that the fluorites crystallized from late stage melts at near solidus temperatures. REE patterns and Eu/Eu*, Rb/Sr and $^{87}Sr/^{86}Sr$ ratios of fluorite are directly inherited from melts with evolving differentiation degrees.

High and variable Tabuleiro granitic fluorite $^{87}Sr/^{86}Sr$ ratios are explained by decay of ^{87}Rb during fractional crystallization of high-Rb/Sr silicic systems with long crystallization time span. Using Cavazzini's equation we have shown that the more radiogenic value recorded by fluorite is consistent with the constrained residence time of the high-silica Long Valley magmatic system (Mahood and Halliday, 1988; Halliday et al., 1989; Christensen and DePaolo, 1993). It permits us to approach the Sr bulk partition coefficients prevailing during the evolution of Tabuleiro granites. The obtained values between 4.7 and 6.0 are consistent with those derived from other evolved high-silica systems by Halliday et al. (1991).

Acknowledgements

We would like to thank Jim Webster and an anonymous reviewer for their useful reviews of an early draft. Marcelle Falcheri and Fabio Caponi (University of Geneva, Switzerland) are thanked for their collaboration during labwork. RS thank Benjamin Carvalho and Clovis Bevilacqua (Mineração Santa Catarina, Grupo Votorantin) and Rui Philipp (Federal University of Rio Grande do Sul, Brazil) for their collaboration during field work. Germano Melo Jr. is thanked for improving the final text. This study was financed by the Swiss National Science Foundation (Grant 20-40575.94); Mineração Santa Catarina; São Paulo State Science Foundation (Fapesp), Brazil, (Grant 89/0254-1); and Federal Science Foundation (CNPq), Brazil, (Grant 400001-89).*[NA]*

References

Batchelor, R.A., Bowden, P., 1985. Petrogenetic interpretation of granitoid rock series using multicationic parameters. Chem. Geol. 48, 43–55.

Bea, F., 1996. Residence of REE, Y, Th and U in granites and crustal protholiths; implications for the chemistry of crustal melts. J. Petrol. 37, 521–552.

Burt, D.M., Bikun, J.V., Christiansen, E.H., 1982. Topaz rhyolites — distribution, origin, and significance for exploration. Econ. Geol. 77, 1818–1836.

Cavazzini, G., 1994. Increase of $^{87}Sr/^{86}Sr$ in residual liquids of high Rb/Sr magmas that evolve by fractional crystallization. Chem. Geol. 118, 321–326.

Charoy, B., Raimbault, L., 1994. Zr, Th and REE rich bitotite differentiates in the A-type granite pluton of Suzhou (Eastern China): the key role of fluorine. J. Petrol. 35, 919–962.

Christensen, J.N., DePaolo, D.J., 1993. Time scales of large volume silicic sytems: Sr isotopic systematics of phenocrysts and glass from the Bishop Tuff, Long Valley, CA. Contrib. Mineral. Petrol. 113, 100–114.

Christiansen, E.H., Burt, D.M., Sheridan, M.F., 1983. The petrogenesis of topaz rhyolite from the Western United States. Contrib. Mineral. Petrol. 83, 16–30.

Clemens, J.D., Holloway, J.R., White, A.J.R., 1986. Origin of A-type granite: experimental constraints. Am. Mineral. 71, 317–324.

Collins, W.K., Beams, S.D., White, A.R.J., Chappel, B.W., 1982. Nature and origin of A-type granites with particular reference to the Southeastern Australia. Contrib. Mineral. Petrol. 80, 189–200.

Congdon, R.D., Nash, W.P., 1988. High-fluorine rhyolite: an eruptive pegmatite magma at the Honeycomb Hills, UT. Geology 16, 1018–1021.

Creaser, A.R., Price, R.C., Wormald, R.J., 1991. A-type granite revisited: assesement of a residual-source model. Geology 19, 163–166.

Evensen, N.M., Hamilton, P.J., O'Nions, R.K., 1978. Rare-earth abundances in chondritic meteorites. Geochim. Cosmochim. Acta 42, 1199–1212.

Flynn, R.T., Burham, W.C., 1978. An experimental determination of rare earth partition coefficients between a chloride containing vapor phase and silicate melts. Geochim. Cosmochim. Acta 42, 685–701.

Fragoso Cesar, A.R.S., Figueiredo, M.C.H., Soliani Jr., E., Faccini, U.F., 1986. In: SBG (Ed.), O batolito Pelotas (Proterozoico Superior/Eo-Palezoico) no escudo do Rio Grande do Sul, Anais 34°Congresso Brasileiro de Geologia, Vol. 3, pp. 1322–1343.

Gerstenberger, H., 1989. Autometasomatic Rb enrichments in highly evolved granites causing lowered Rb–Sr isochron intercepts. Earth Planet. Sci. Lett. 93, 65–75.

Halliday, A.N., Mahood, G.A., Holden, P., Metz, J.M., Dempster, T.J., Davidson, J.P., 1989. Evidence for long residence times of rhyolitic magma in the Long Valley magmatic system: the isotopic record in precaldera lavas of Glass Mountain. Earth Planet. Sci. Lett. 94, 274–309.

Halliday, A.N., Davidson, J.P., Hildreth, W., Holden, P., 1991. Modelling the petrogenesis of high Rb/Sr silicic magmas. Chem. Geol. 92, 107–114.

Holtz, F., Dingwell, D., Behrens, H., 1993. Effects of F, B_2O_3 and P_2O_5 on the solubility of water in haplogranitic melts compared to natural silicate melts. Contrib. Mineral. Petrol. 113, 492–501.

Horbach, R., Marimon, R., 1982. Contribuição a geologia do distrito de fluorita de Santa Catarina. Boletim Técnico, Série Geologia, Projeto RADAMBRASIL, 1P.104, Salvador.

Huspeni, J.R., Kesler, S.E., Ruiz, J., Tuta, Z., Sutter, J.F., Jones, L.M., 1984. Petrology and geochemistry of rhyolites associated with tin mineralization in northern Mexico. Econ. Geol. 79, 87–105.

Johnston, C., Chappel, B.W., 1992. Topaz-bearing rocks from Mount Gibson, North Queensland, Australia. Am. Mineral. 77, 303–313.

Keppler, H., Wyllie, J., 1991. Partioning of Cu, Sn, Mo, W, U, and Th between melt and aqueos fluid in the systems haplogranite–H_2O–HCl and haplogranite–H_2O–HF. Contrib. Mineral. Petrol. 101, 139–150.

Kirchner, C.A., Morgental, A., 1983. Projeto fluorita no sudeste de Santa Catarina. Relatorio preliminar, Etapa 3 — Pesquisa de Metodos. DNPM/CPRM, Porto Alegre, 108 pp., unpublished.

Koster Van Gross, A.F.K., Wyllie, P.J., 1969. Melting relationships in the system $NaAlSi_3O_8$–NaF–H_2O at 1 kilobars pressure, with petrological applications. J. Geol. 77, 581–605.

Lachenbruch, A.H., Sorey, M.L., Lewis, R.E., Sass, J.H., 1976. The near-surface hydrothermal regime of long Valley caldera. J. Geophys. Res. 81, 763–784.

Mahood, G.A., Halliday, A.N., 1988. Generation of high-silica rhyolite: a Nd, Sr, and O isotopic study of Sierra La Primavera, Mexican Neovolcanic Belt. Contrib. Mineral. Petrol. 100, 183–191.

Mineyev, D.A., 1969. Spectrum of lanthanoïdes in ores of rare earths deposits of different genetic types. Geol. Rev. 11, 965–971.

Marchand, L., Joseph, D., Touray, J.C., 1976. Critères d'analyse géochimique des gisements de fluorine basés sur l'étude de la distribution des lanthanides — application au gite du Maine. Mineral. Deposita 11, 357–379.

Nash, W.P., 1993. Fluorine iron biotite from the Honeycomb Hills rhyolite, Utah: The halogen record of decompression in silicic magma. Am. Mineral. 78, 1031–1040.

Price, J.G., Castor, S.B., Miller, D.M., 1992. Highly radioactive topaz rhyolite of the Toano Range, Northeastern Nevada. Am. Mineral. 77, 1067–1073.

Sallet, R., 1988. Essai de caractérisation d'une suite plutonique monzonitique d'après la chimie des biotites (F, Mg et Fe): l'exemple des granitoïdes du Sud du Massif Catarinense, Brésil. C.R. Acad. Sci. Paris 307 (II), 379–385.

Sallet, R., 1999. Fluorine as a tool in the petrogenesis of quartz-bearing magmatic associations: applications of an improved F–OH biotite–apatite thermometer grid. Lithos (in press).

Sallet, R., Ferreira, A.C., Fragoso Cesar, A.R., Monteiro, R., Machado, R., 1989. O arcabouço granítico transalcalino tardi-orogênico do Batólito Pelotas (sul do Brasil e Uruguai) e sua potencialidade para mineralizações de Fluorita. Acta Geologica Leopoldensia 30 (13), 213–228.

Sallet, R., Ferreira, A.C., Sabatier, H., 1990. Petrografia e geoquímica dos granitóides do sul do distrito de fluorita de Santa Catarina. Folhas Jaguaruna et Tubarão. In: SBG (Ed.), Anais 36°Congresso Brasileiro de Geologia, Vol. 4, pp. 1793–1806.

Sallet, R., Moritz, R., Fontignie, D., 1996. $^{87}Sr/^{86}Sr$ systematics at the post-Jurassic Santa Catarina Fluorite Districts, Brazil. Genetic Model and age implications. In: SBG (Ed.), Anais 39°Congresso Brasileiro de Geologia, IGCP 342 Symposium Age and Isotopes of South American Ores, Vol. 7, pp. 328–332.

Sallet, R., Moritz, R., Sabatier, H, 1997. Geochemistry of the Tabuleiro high-silica fluorite granites: Pelotas Batholith, southern Brazil. Potential for Sn–Mo Mineralizations. In: Papunen, H. (Ed.), Proceedings of the fourth biennial SGA meeting. Balkema, Rotterdam, pp. 667–670.

Spera, F., 1979. Thermal evolution of plutons: a parameterized approach. Science 297, 299–301.

Tsareva, G.M., Naumov, V.B., Kovalenko, V.I., Tsepin, A.I., Babanskiy, A.D., 1992. Melt-inclusion data on the composition and crystallization conditions of the Spor Mountain topaz rhyolite. Geochemistry International 29, 93–102.

Webster, J.D., 1990. Partitioning of F between H_2O and CO_2 fuids and topaz rhyolite melt. Contrib. Mineral. Petrol. 104, 424–438.

Webster, J.D., Duffield, W.A., 1991. Volatiles and lithophiles elements in Taylor Creek Rhyolite: Constraints from glass inclusions analysis. Am. Mineral. 76, 1628–1645.

Webster, J.D., Duffield, W.A., 1994. Extreme halogen abundances in tin-rich magma of the Taylor Creek-Rhyolite, NM. Econ. Geol. 89, 840–850.

Webster, J.D., Holloway, J.R., Hervig, R.L., 1987. Phase equilibria of Be, U and F-enriched vitrophyre from Spor Mountain, UT. Geochim. Cosmochim. Acta 51, 389–402.

Whalen, J.B., Currie, K.L., Chappel, B.W., 1987. A-type granites: geochemical characteristics, discrimination and petrogenesis. Contrib. Mineral. Petrol. 95, 407–419.